Communications to SIMAI Congress,
ISSN 1827-9015, Vol. 2 (2007)

DOI: 10.1685/CSC06166

ON A MATHEMATICAL MODEL OF TWISTED MULTIWALL CARBON NANOTUBES

A. DI CARLO* and L. TERESI†

SMFM@DiS, Università "Roma Tre",
Via Corrado Segre 4/6, I-00146 Roma, Italy
**E-mail: adicarlo@mac.com*
†*E-mail: teresi@uniroma3.it*

P. PODIO GUIDUGLI

Dip. Ingegneria Civile,
Università di Roma TorVergata,
Viale Politecnico, 1 I-00133 Roma, Italy
E-mail: ppg@uniroma2.it

Abstract.

We propose a continuum theory of twisted MWCNTs, in which interwall interactions depend significantly on defect density. We envisage various sorts of defect populations, one of them being nucleated at the outermost wall due to chromium deposition during fabrication; when triggered by repeated twisting cycles, defects transform and migrate in either the circumferential or the inward radial direction. We expect our model to account for all of the seemingly contradictory experimental facts reported in Refs. 1–5; the relative numerical tests are on their way.

Keywords: Twisted MWCNTs, NEMS, Continuum Modelling.

1. Introduction

In recent years, individual MultiWall Carbon NanoTubes (MWCNTs) have been incorporated into various Nano-ElectroMechanical Systems (NEMS), to serve as torsional oscillators[1,2,3] or to produce rotor bearings.[4,5] When fabricating these devices, first chromium then gold are thermally evaporated onto the nanotube, to manufacture metal pads strongly anchored to its outermost wall. In spite of its practical success—or, possibly, just because of it—the detailed mechanisms of the interaction of Cr atoms with the C lattice structure are to our knowledge largely unexplored.

1.1. *Experimental background*

Nanoscale oscillators with MWCNTs working as torsion springs have been fabricated by the Nanoscale Science Research Group (NSRG) at the University of North Carolina-Chapel Hill.[1] The torsion stiffness was measured by an atomic force microscope mounted inside the chamber of a Scanning Electron Microscope (SEM). All tested devices exhibited a sizeable increase in torsion stiffness, roughly correlated with the total number of twisting cycles. After about 500 small-amplitude twisting cycles (with an estimated average inwall

strain smaller than 0.01), the stiffness of an individual MWCNT saturated to a value 12 times larger than its initial value.[2] However, when the stiffness of a series of such oscillators was measured after they had been driven on resonance, thus undergoing a much larger number of twisting cycles, the outcome was puzzling: only half of the times the measured stiffness matched the expected saturation value, otherwise taking lesser values, mostly near the expected minimum.[3] Roughly speaking, in these experiments an enigmatic interwall-coupling mechanism was either linking all of the shells strongly or none at all (or nearly so).

The Zettl Research Group at the University of California-Berkeley[4] and, independently, the Laboratoire de Physique de la Matière Condensée at the École Normale Supérieure, Paris,[5] have fabricated NEMS where an individual MWCNT, quite similar to those employed by the NSRG and suitably engineered, works as a rotary bearing. Needless to say, interwall sliding occurs; the observed interwall friction is very small,[a] and does not increase during operation; hence, conceivably, no elastic links form between sliding walls. Interestingly, the Zettl Group has obtained a nanorotor from a metal plate mounted on a MWCNT by breaking the outer wall(s) by a few twisting cycles of large amplitude.

Recently, a torsional pendulum based on a single-walled carbon nanotube has been fabricated.[6] Such a device is obviously free of the intricacies of interwall interactions, and may have other definite advantages over MWCNT-based NEMS. However, understanding the elusive mechanisms of interwall coupling in MWCNTs not only is worthwhile *per se* but might also prove important to open the way to new applications.

1.2. *Rationale*

The seeming contradiction between the experimental observations reported in Refs. 1–3 and those in Refs. 4, 5 prompts the conjecture that defects created by metal deposition on the carbon structure are crucial in determining both the fragile behaviour under a few large twists and the ratcheting effect under many small ones. One is also led to presume that defects can undergo various competing transformations. The purpose of this note is to contribute to sort out the accompanying variety of interwall interactions.

We speculate that the basic mechanism behind progressive interwall coupling is the formation of *bridging defects*, that is, of covalent bonds between adjacent walls created as a consequence of the inward defect migration triggered by repeated twisting cycles. Our speculations are substantiated by the simulations reported in Refs. 7 and 8, based on Density Functional Theory (DFT) and the Adaptive Intermolecular Reactive Empirical Bond Order (AIREBO) model, respectively: the work of Telling *et al.*[7] indicates that vacancy defects do not simply modify inwall interactions—as is commonly believed—but are able to bridge the interwall gap; Huhtala *et al.*[8] find that a small number of defects can enhance a MWCNT's interwall mechanical properties considerably, while changing its inwall properties in a negligible way.

We surmise that pristine defects in the outer wall are created by the interaction of Cr atoms with the C lattice structure when chromium is evaporated onto the nanotube for

[a]Bourlon *et al.*[5] have applied a slowly increasing bias voltage between the plate and one stator electrode of a device similar to the one shown in Fig. 1 (right), and measured the minimum voltage required to make the plate move. The value of 0.85 ± 0.15 MPa for the static friction (interwall force per unit area) has been obtained by estimating the electrostatic couple applied to the plate and assuming it to be balanced by a uniform interwall shear stress.

fabricating the device. Preliminary results from a DFT study[9] of Cr atoms and dimers on graphene seem to support this conjecture.

Hereafter, we propose a mesomechanical theory of twisted MWCNTs, in which defect populations of different sorts, when triggered by repeated twisting cycles, evolve and interact with one another, migrating in either the circumferential or the inward radial direction. Improving on an earlier and more restricted theoretical proposal of ours,[10] the present model does not contain any *ad hoc* growth law for the interwall coupling; we believe it provides a simple mesoscopic format to account for all of the seemingly contradictory experimental facts reported in Refs. 1–5. In the numerical computations we are currently implementing, the models parameters are tuned by importing both data measured on devices, such as those available in Refs. 1–5, and numerical results from electronic structure calculations like the ones in Refs. 7–9.

2. Kinematics

To fix ideas, we think of a device consisting of a single MWCNT, anchored at both ends and carrying a centred plate. We let the CNT have $n{+}1$ walls, labelled from outside in with integers ranging from 0 to n. There are then n interwalls, the i-th of them being sandwiched between the $(i{-}1)$-th and i-th walls. To write formulae featuring summations over all walls and interwalls more compactly, we find it expedient to introduce a fictitious outermost 0-th interwall. We refer to the 'tube' as to the segment of MWCNT spanning from an anchor to the suspended plate (see Fig. 1), and label its left (anchor) and right (plate) ends by a minus ($-$) and a plus ($+$), respectively.

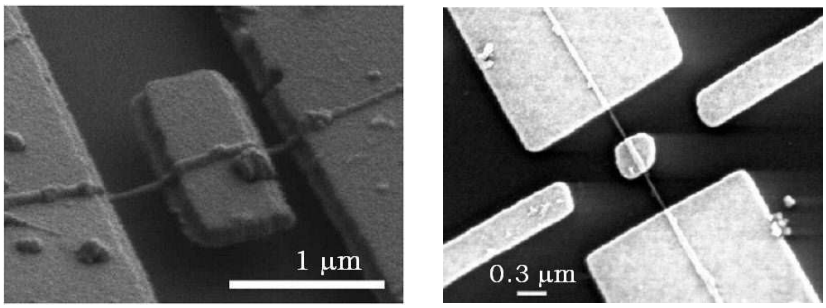

Fig. 1. Two MWCNT-based NEMS: the straight CNT buried underneath produces the mounds one sees on the gold surface: (left) Torsional oscillator fabricated by the NSRG at Chapel Hill (SEM image reproduced from Ref. 2); (right) Rotational actuator constructed by the Zettl group at Berkeley (SEM image from Ref. 4, taken in an advanced stage of fabrication, just prior to removal of ∼500 nm of the underlying SiO_2 bed, to provide the clearance the rotor plate needs to spin.

The **angle of rotation** of the e-end of the i-th wall with respect to the anchor is denoted by φ_i^e ($e = \mp$); typically, of all angles φ_i^e, only φ_0^- is null and φ_0^+ equals the rotation angle of the paddle. The **angle of twist** θ_i of the i-th wall and the **interwall shear** γ_i^e at the e-end of the i-th interwall are defined as the differences:

$$\theta_i := \varphi_i^+ - \varphi_i^- , \qquad \gamma_i^e := \varphi_{i-1}^e - \varphi_i^e , \tag{1}$$

it being understood that $\theta_{-1}^e := \theta_0^e$, whence $\gamma_0^e = 0$; the **relative interwall shear** at time t with respect to time τ, ${}^r\gamma_i^e(\tau, t)$, is defined accordingly:

$${}^r\gamma_i^e(\tau, t) := \gamma_i^e(t) - \gamma_i^e(\tau) . \tag{2}$$

We envisage *four* types of **defects**, all of them concentrated for simplicity at the tube ends where exposition to chromium takes place during fabrication, quantified through their *circumferential densities* (number of defects per unit circumferential length). Specifically, we let a_i^e, w_i^e, and p_i^e denote the densities of **Cr-activated defects** (*a-defects*, for short), **inwall bond-breaking defects** (*w-defects*), and **passivated defects** (*p-defects*) at the $e-$end of the i-th wall; moreover, we denote by b_i^e the density of **gap-bridging defects** (*b-defects*) at the $e-$end of the i-th interwall.

A **process** of the tube is an ordered m-tuple ($m = 10\,n$) of smooth functions of time:

$$\left(\varphi_i^e \,; a_i^e, w_i^e, p_i^e, b_i^e \,\middle|\, i = 0, \dots, n\,,\ e = \mp \right), \quad \text{with} \quad b_0^e = 0, \tag{3}$$

delivering the current values of our *state variables*, the rotation angles (our gross descriptors) and the defect densities (our order parameters). A **test velocity** is an m-tuple of reals, denoted

$$\left(\omega_i^e \,; \alpha_i^e, \varpi_i^e, \pi_i^e, \beta_i^e \,\middle|\, i = 0, \dots, n\,,\ e = \mp \right); \tag{4}$$

in particular, the **velocity realized** along a given process (3) at time t is characterized by the equalities:

$$\omega_i^e = \dot{\varphi}_i^e(t)\,, \quad \alpha_i^e = \dot{a}_i^e(t)\,, \quad \varpi_i^e = \dot{w}_i^e(t)\,, \quad \pi_i^e = \dot{p}_i^e(t)\,, \quad \beta_i^e = \dot{b}_i^e(t) \tag{5}$$

(a superposed dot signals time differentiation).

3. Dynamics

3.1. *Working and balance*

We assume the **working** expended on a general test velocity (4) to be[b]:

$$\sum_{i=0}^{n} \sum_{e=\mp} \Big[\left(\mathrm{M}_i^e - e\mathrm{T}_i \right) \omega_i^e - \mathrm{C}_i^e \left(\omega_{i-1}^e - \omega_i^e \right) + \mathrm{A}_i^e\, \alpha_i^e + \mathrm{W}_i^e\, \varpi_i^e + \mathrm{P}_i^e\, \pi_i^e + \mathrm{B}_i^e\, \beta_i^e \Big], \tag{1}$$

where T_i denotes the **wall torque**, C_i^e the **interwall couples**, and $\mathrm{A}_i^e, \mathrm{W}_i^e, \mathrm{P}_i^e, \mathrm{B}_i^e$ the **remodelling actions** on a-, w-, p- and b-defects, respectively; the **applied end couples** M_i^e are the only external actions, implying that the only excitable degrees of freedom of the tube are the rotation angles of its walls (we believe the experimental conditions to be well represented by the position $\mathrm{M}_i^e = 0$ for $i \neq 0$, *i.e.*, by assuming that only the outermost wall interacts with the anchor and the plate). On requiring that the working be null whatever the test velocity, we obtain the following m **balance equations**:

$$-e\mathrm{T}_i + \mathrm{C}_i^e - \mathrm{C}_{i+1}^e + \mathrm{M}_i^e = 0\,; \quad \mathrm{A}_i^e = 0\,, \quad \mathrm{W}_i^e = 0\,, \quad \mathrm{P}_i^e = 0\,, \quad \mathrm{B}_i^e = 0\,. \tag{2}$$

[b]It is intended that, when used as coefficients, the labels $\mp$ stand for ∓ 1.

3.2. *Constitutive mappings*

Although, in principle, the constitutive mappings delivering the internal actions entering the balance equations Eq. (2) should all depend on one and the same list of state variables, experience and empirical evidence help motivating the following special—but not too special!—choice:

$$
\begin{aligned}
\mathrm{T}_i(t) &= \widehat{\mathrm{T}}_i\left(\theta_i(t), w_i^-(t), w_i^+(t), a_i^-(t), a_i^+(t)\right),\\
\mathrm{C}_i^e(t) &= \widehat{\mathrm{C}}_i^e\left((\varphi_{i-1}^e - \varphi_i^e)^t, (b_i^e)^t\right),\\
\mathrm{A}_i^e(t) &= \widehat{\mathrm{A}}_i^e\left(\theta_i^t, w_i^-(t), w_i^+(t), a_i^e(t); \dot{a_i^e}(t)\right),\\
\mathrm{W}_i^e(t) &= \widehat{\mathrm{W}}_i^e\left(\theta_i(t), w_i^-(t), w_i^+(t), a_i^-(t), a_i^+(t); \dot{w_i^e}(t)\right),\\
\mathrm{P}_i^e(t) &= \widehat{\mathrm{P}}_i^e\left(\dot{p_i^e}(t)\right),\\
\mathrm{B}_i^e(t) &= \widehat{\mathrm{B}}_i^e\left(\dot{b_i^e}(t)\right),
\end{aligned}
\tag{3}
$$

where f^t denotes the *history up to time* t of the quantity f, namely, the mapping $s \mapsto f^t(s) := f(t-s)$, $0 \le s \le t$.

3.3. *Free energy*

We take the **free energy** available to the system to be, at any time $t \ge 0$,

$$
\begin{aligned}
\Psi(t) = \sum_{i=0}^{n} \Bigg[\tfrac{1}{2}\,\mathrm{K}_i(t)\,\theta_i(t)^2 + \sum_{e=\mp} \Bigg(\tfrac{1}{2}\,\mathrm{c}_i \int_0^t \dot{b_i^e}(\tau)\,{}^r\gamma_i^e(\tau,t)^2\,d\tau + \\
\psi_i^a\,a_i^e(t) + \psi_i^w\,w_i^e(t) + \psi_i^p\,p_i^e(t) + \psi_i^b\,b_i^e(t) \Bigg) \Bigg].
\end{aligned}
\tag{4}
$$

Here K_i, the **torsional stiffness** of the i-th wall, depends in a crucial way on the densities of a- and w-defects:

$$
\mathrm{K}_i(t) := \mathrm{K}_i^0\big(w_i^-(t), w_i^+(t)\big)\Big(1 + \kappa_i\left(a_i^-(t) + a_i^+(t)\right)\Big). \tag{5}
$$

In particular, the **mean-field stiffness** K_i^0 is supposed to attain a smooth (and—we presume—rather shallow) maximum at $(0,0)$, the torsional stiffness of an intact wall, and to *decrease* to null for large enough w-defect densities. Moreover, the energy content of a-defects is supposed to *increase* when walls are twisted, an effect measured by the *small positive* coefficients κ_i (we have reasons to believe that

$$
\mu_i(t) := 1 + \kappa_i\left(a_i^-(t) + a_i^+(t)\right) \approx 1 \tag{6}
$$

under experimental conditions). But, no matter how small on the scale of the entire wall, the energy associated with these terms plays a key role in the model, since it can be large enough on the scale of defects to trigger their transformation. The energy barriers involved in an individual transition should be of the order of magnitude of 1 eV. As to length scales, the size of an individual defect is of the order of magnitude of the hexagonal C-lattice cell ($\sim$0.25 nm); this is to be compared with the distance h between two adjacent walls ($h = 0.34$ nm, the 'graphite gap'), the tube's outer diameter (from 10 to 40 nm), and the tube's suspended length (the anchor-to-plate span, from 0.2 to 1.0 μm).

The **specific defect energies** $\psi_i^a, \psi_i^w, \psi_i^p$, and ψ_i^b, measure the free-energy contribution of each type of defects in the case of either an *untwisted* wall ($\theta_i(t)=0$) or an *unsheared* interwall (${}^r\gamma_i^e(\cdot,t)=0$). Note that, according to (4), the energy content of a b-defect *increases* when the interwall it bridges is sheared, in a manner proportional to the square of the relative shear between the present time and the time the bridge was created. Since b-defects are supposed to stay once created,[c] the (positive) quantity $\dot{b}_i^e(\tau)\,\varepsilon$ gauges the number of b-defects created in a short time lapse $\varepsilon>0$ around time τ, and the product $\mathrm{c}_i\,\dot{b}_i^e(\tau)\,\varepsilon$ accounts for their contribution to the **shear stiffness** of the i-th interwall. Supported by Ref. 8, we believe the coefficients c_i to be large, so as to ensure that few defects give a sizeable contribution to shear stiffness.

3.4. *Dissipation inequality & defect kinetics*

We restrict the choice of the constitutive mappings (3) by requiring that, at each time t (dropped from the notation), the following dissipation inequality be satisfied :

$$\dot{\Psi} \le \sum_{i=0}^{n} \Bigg[\widehat{\mathrm{T}}_i(\ell)\,\dot{\theta}_i + \sum_{e=\mp} \Bigg(\widehat{\mathrm{C}}_i^e(\ell)\,\dot{\gamma}_i^e - \Big(\widehat{\mathrm{A}}_i^e(\ell)\,\dot{a}_i^e + \widehat{\mathrm{W}}_i^e(\ell)\,\dot{w}_i^e + \widehat{\mathrm{P}}_i^e(\ell)\,\dot{p}_i^e + \widehat{\mathrm{B}}_i^e(\ell)\,\dot{b}_i^e \Big) \Bigg) \Bigg], \tag{7}$$

for all admissible processes (here ℓ is shorthand for a list of variables that varies case by case, as detailed in Eq. (3)). With a view toward deriving the implications of this requirement, we evaluate the time derivative of the free energy (4) along a process (3):

$$\dot{\Psi} = \sum_{i=0}^{n} \Bigg[\mathrm{K}_i\,\theta_i\,\dot{\theta}_i + \sum_{e=\mp} \Bigg(\mathrm{c}_i\,\Gamma_i^e\,\dot{\gamma}_i^e + \tfrac{1}{2}\,\theta_i^2 \Big(\partial_e \mathrm{K}_i\,\dot{w}_i^e + \mathrm{K}_i^0\big(w_i^-, w_i^+\big)\,\kappa_i\,\dot{a}_i^e \Big) + \psi_i^a\,\dot{a}_i^e + \psi_i^w\,\dot{w}_i^e + \psi_i^p\,\dot{p}_i^e + \psi_i^b\,\dot{b}_i^e \Bigg) \Bigg], \tag{8}$$

where

$$\Gamma_i^e(t) := \int_0^t \dot{b}_i^e(\tau)\,{}^r\gamma_i^e(\tau,t)\,d\tau \tag{9}$$

is the **effective interwall shear** at time t, the symbol ∂_e denotes differentiation with respect to the e-labelled argument of K_i^0:

$$\partial_e \mathrm{K}_i(t) := \mu_i(t)\,(\partial_e \mathrm{K}_i^0)\Big|_{\left(w_i^-(t),w_i^+(t)\right)}, \tag{10}$$

and use of (6) has been made.

[c] In principle, severely stressed interwall bridges might break down. However, we are not aware of any experiment in which a MWCNT was severely twisted—as in Ref. 4—*after* having been subjected to many gentler twisting cycles—as in Ref. 1–3. Hence, for the time being, we have not implemented interwall-bridge breakage in our model.

Notice that we associate dissipation only with defect evolution, *i.e.*, with the time rate of change of defect densities (see Eq. (3)). Accordingly, we split each of the constitutive mappings $\widehat{\mathrm{A}}_i^e, \widehat{\mathrm{W}}_i^e, \widehat{\mathrm{P}}_i^e$, and $\widehat{\mathrm{B}}_i^e$ into the sum of *equilibrium* and *dissipation* components:

$$
\begin{aligned}
&\widehat{\mathrm{A}}_i^e\Big(\theta_i^t, w_i^-(t), w_i^+(t), a_i^e(t); \dot{a_i^e}(t)\Big) = \\
&\qquad \overset{equ}{\mathrm{A}}{}_i^e\Big((\theta_i, w_i^-, w_i^+, a_i^e)\big|_t\Big) - \overset{dis}{\mathrm{A}}{}_i^e\Big((\theta_i, w_i^-, w_i^+, a_i^e)\big|_t\Big)\,, \\
&\text{with} \qquad \overset{equ}{\mathrm{A}}{}_i^e\Big((\theta_i, w_i^-, w_i^+, a_i^e)\big|_t\Big) := \widehat{\mathrm{A}}_i^e\Big(\theta_i^t, (w_i^-, w_i^+, a_i^e)\big|_t; 0\Big)
\end{aligned}
\tag{11}
$$

and so forth. With this, on substituting the expression (8) of $\dot{\Psi}$ into (7), we exploit that inequality *à la* Coleman-Noll and obtain the following representation results for wall torques and interwall couples:

$$
\begin{aligned}
\mathrm{T}_i(\ell) &= \overline{\mathrm{T}}_i(\ell) = \mathrm{K}_i(t)\,\theta_i(t)\,, \\
\mathrm{C}_i^e(\ell) &= \overline{\mathrm{C}}_i^e(\ell) = \mathrm{c}_i\,\Gamma_i^e(t)\,,
\end{aligned}
\tag{12}
$$

and for the equilibrium components of defect-remodelling actions:

$$
\begin{aligned}
\overset{equ}{\mathrm{A}}{}_i^e(\ell) &= -\psi_i^a - \tfrac{1}{2}\,\mathrm{K}_i^0(w_i^-, w_i^+)\big|_t\,\kappa_i\,\theta_i(t)^2, \\
\overset{equ}{\mathrm{W}}{}_i^e(\ell) &= -\psi_i^w - \tfrac{1}{2}\,\partial_e\mathrm{K}_i(t)\,\theta_i(t)^2, \\
\overset{equ}{\mathrm{P}}{}_i^e(\ell) &= -\psi_i^p\,, \\
\overset{equ}{\mathrm{B}}{}_i^e(\ell) &= -\psi_i^b\,.
\end{aligned}
\tag{13}
$$

We are left with the following **reduced dissipation inequality**:

$$
\sum_{i=0}^{n}\sum_{e=\mp}\Big(\overset{dis}{\mathrm{A}}{}_i^e\,\dot{a}_i^e + \overset{dis}{\mathrm{W}}{}_i^e\,\dot{w}_i^e + \overset{dis}{\mathrm{P}}{}_i^e\,\dot{p}_i^e + \overset{dis}{\mathrm{B}}{}_i^e\,\dot{b}_i^e\Big) \le 0\,,
\tag{14}
$$

where we regard as admissible only those time rates of defect densities which satisfy the conditions:

$$
\dot{w}_i^e \ge 0\,, \quad \dot{p}_i^e \ge 0\,, \quad \dot{b}_i^e \ge 0\,,
\tag{15}
$$

$$
\dot{a}_i^e = \big(\rho_i\,\dot{b}_i^e - \dot{b}_{i+1}^e\big) - \big(\dot{w}_i^e + \dot{p}_i^e\big)\,,
\tag{16}
$$

with $\dot{b_0^e} = \dot{b_{n+1}^e} = 0$. Inequalities (15) formalize the hypothesis that w-, p- and b-defects, once formed, neither decay nor change type. Equation (16) tells us that w- and p-defects can be nucleated only by annihilating a corresponding amount of a-defects; and that the formation of a b-defect between two adjacent walls entails the migration of an a-defect from the outer to the inner wall, with the factor

$$
\rho_i := \frac{r_{i-1}}{r_i} = 1 + \frac{h}{r_i}
\tag{17}
$$

accounting for the difference between the radii of walls i and i–1. If we further assume that the kinetics of w-, p-, and b-defects are otherwise uncoupled, it turns out that inequality

(14) is satisfied if and only if there are *nonnegative*-valued **defect-reluctance** functions $\overset{w}{\mathrm{D}}{}^e_i, \overset{p}{\mathrm{D}}{}^e_i, \overset{b}{\mathrm{D}}{}^e_i$, such that

$$
\begin{aligned}
\overset{dis}{\mathrm{W}}{}^e_i(\ell) - \overset{dis}{\mathrm{A}}{}^e_i(\ell) &= -\overset{w}{\mathrm{D}}{}^e_i(\ell)\, \dot{w}^e_i(t)\,, \\
\overset{dis}{\mathrm{P}}{}^e_i(\ell) - \overset{dis}{\mathrm{A}}{}^e_i(\ell) &= -\overset{p}{\mathrm{D}}{}^e_i(\ell)\, \dot{p}^e_i(t)\,, \\
\overset{dis}{\mathrm{B}}{}^e_i(\ell) + \rho_i \overset{dis}{\mathrm{A}}{}^e_i(\ell) - \overset{dis}{\mathrm{A}}{}^e_{i-1}(\ell) &= -\overset{b}{\mathrm{D}}{}^e_i(\ell)\ \dot{b}^e_i(t)\,,
\end{aligned}
\tag{18}
$$

and that inequalities (15) and the nonnegativity requirement on a-defect density are satisfied if

$$
\overset{w}{\mathrm{D}}{}^e_i(\ell) = \infty \ \text{ whenever } \ \dot{w}^e_i(t) < 0 \quad \text{or} \quad a^e_i(t) = 0 \ \&\ \dot{a}^e_i(t) < 0\,,
\tag{19}
$$

et similiter for $\overset{p}{\mathrm{D}}{}^e_i$ and $\overset{b}{\mathrm{D}}{}^e_i$ (note that inequalities (15) ensure that w^e_i, p^e_i, b^e_i stay nonnegative along whatever process in which they have nonnegative initial values).

4. Evolution Laws

Combination of the constitutive information in Eqs. (13) and (18) with the balance laws (2) gives the latter their evolutionary form.

The **defect evolution laws**, the main novelty of our model, read as follows:

$$
\begin{aligned}
\overset{w}{\mathrm{D}}{}^e_i(\ell)\, \dot{w}^e_i &= \big(\psi^a_i + \tfrac{1}{2}\,\mathrm{K}^0_i\big(w^-_i, w^+_i\big)\,\kappa_i\,\theta^2_i\big) - \big(\psi^w_i + \tfrac{1}{2}\,\partial_e \mathrm{K}_i\,\theta^2_i\big)\,, \\
\overset{p}{\mathrm{D}}{}^e_i(\ell)\, \dot{p}^e_i &= \big(\psi^a_i + \tfrac{1}{2}\,\mathrm{K}^0_i\big(w^-_i, w^+_i\big)\,\kappa_i\,\theta^2_i\big) - \psi^p_i\,, \\
\overset{b}{\mathrm{D}}{}^e_i(\ell)\ \dot{b}^e_i &= \Big(\psi^a_{i-1} + \tfrac{1}{2}\,\mathrm{K}^0_{i-1}\Big(w^-_{i-1}, w^+_{i-1}\Big)\,\kappa_{i-1}\,\theta^2_{i-1}\Big) - \\
&\quad \big(\rho_i\,\big(\psi^a_i + \tfrac{1}{2}\,\mathrm{K}^0_i\big(w^-_i, w^+_i\big)\,\kappa_i\,\theta^2_i\big) + \psi^b_i\big)\,.
\end{aligned}
\tag{1}
$$

The specific defect energies $\psi^a_i, \psi^w_i, \psi^p_i$, and ψ^b_i, measure the energetic content of defects *per unit circumferential density*. Now, it is reasonable to assume that the energy of an *individual* defect, whatever its type, is independent of its location. Since defect size, being related to the size of a C-lattice cell, is also independent of location, the densities ψ^a_i, ψ^w_i, and ψ^p_i scale with the radius r_i as follows with respect to the 0-th wall:

$$
\psi^a_i = \frac{r_i}{r_0}\,\psi^a_0 \quad \text{etc.}
\tag{2}
$$

The specific energy of b-defects may be scaled analogously, this time with respect to the first interwall:

$$
\psi^b_i = \frac{r_{i-1} + r_i}{r_0 + r_1}\,\psi^b_1 = \frac{r_i + h/2}{r_0 - h/2}\,\psi^b_1\,.
\tag{3}
$$

The same argument applies to the coefficients κ_i regulating the energy increase of a-defects when strained (see Eq. (5)), leading to:

$$
\kappa_i = \frac{r_i}{r_0}\,\kappa_0\,.
\tag{4}
$$

The torsional stiffness of an intact wall scales with the 3rd power of its radius:

$$
\mathrm{K}^{00}_i := \mathrm{K}^0_i(0,0) = 2\pi\, G\, h\, r^3_i\,,
\tag{5}
$$

where $G \approx 500$ GPa is the nominal *inwall shear modulus*.[3,11] It seems sensible to assume that

$$\mathrm{K}_i^0(w^-, w^+) = \mathrm{K}_i^{00}\,\delta(w^-, w^+)\,, \tag{6}$$

with δ a **damage function**, the same for all walls, such that $\delta(0,0) = 1$ and $\partial_e\delta < 0$ everywhere except in $(0,0)$, where its derivatives $\partial_e\delta$ are null. In fact, what matters here is the ratio of the number of inwall bond-breaking defects (w-defects) to the total number of circumferential bonds, and this ratio is, for the i-th wall, proportional to the density w_i^e.

Passing from energetics to kinetics, it is reasonable to assume that also the energy dissipated in the formation of an individual defect of a given type does not depend on location. Therefore, we get

$$\overset{w}{\mathrm{D}}{}_i^e(\ell) = \frac{r_i}{r_0}\,\overset{w}{\mathrm{D}}{}_0(\ell)\,,\ \overset{p}{\mathrm{D}}{}_i^e(\ell) = \frac{r_i}{r_0}\,\overset{p}{\mathrm{D}}{}_0(\ell)\,,\ \overset{b}{\mathrm{D}}{}_i^e(\ell) = \frac{r_i+h/2}{r_0-h/2}\overset{b}{\mathrm{D}}{}_1(\ell)\,. \tag{7}$$

Under assumptions (2)–(7), Eqs. (1) take on the form:

$$\begin{aligned}
\overset{w}{\mathrm{D}}{}_0(\ell)\,\dot{w}_i^e &= \psi_0^a - \psi_0^w + \tfrac{1}{2}\,\mathrm{K}_i^{00}\Big(\kappa_0\,\delta(w_i^{\mp}) - \frac{r_0}{r_i}\,\mu_i\,(\partial_e\delta)|_{w_i^{\mp}}\Big)\,\theta_i^2\,,\\
\overset{p}{\mathrm{D}}{}_0(\ell)\,\dot{p}_i^e &= \psi_0^a - \psi_0^p + \tfrac{1}{2}\,\mathrm{K}_i^{00}\,\kappa_0\,\delta(w_i^{\mp})\,\theta_i^2\,,\\
\overset{b}{\mathrm{D}}{}_1(\ell)\ \dot{b}_i^e &= -\psi_1^b + \tfrac{1}{2}\,\widetilde{\rho}_i\,\kappa_0\Big(\mathrm{K}_{i-1}^{00}\,\delta(w_{i-1}^{\mp})\,\theta_{i-1}^2 - \mathrm{K}_i^{00}\,\delta(w_i^{\mp})\,\theta_i^2\Big),
\end{aligned} \tag{8}$$

where the following shorthands have been used:

$$\delta(w^{\mp}) := \delta(w^-, w^+)\,, \qquad \widetilde{\rho}_i := \frac{1-h/2\,r_0}{1+h/2\,r_i}\,\rho_i\,. \tag{9}$$

Equations (8) are to be coupled with Eq. $(2)_1$, which, after substitution of Eqs. $(13)_{1,2}$, (9), (1) and (2), may be rewritten in rate form as follows:

$$\begin{aligned}
&-\,e\,\mathrm{K}_i^{00}\sum_{l=\mp}\Big(l\,\delta(w_i^{\mp})\,\mu_i\,\dot{\varphi}_i^l + \kappa_i\,\theta_i\,\delta(w_i^{\mp})\,\dot{a}_i^l + \mu_i\,\theta_i\,(\partial_l\,\delta)\big|_{w_i^{\mp}}\,\dot{w}_i^l\Big)\\
&+\,\frac{\mathrm{c}_1}{r_0-h/2}\Bigg((r_i+h/2)\,b_i^e\,\dot{\varphi}_{i-1}^e + (r_i-h/2)\,b_{i+1}^e\,\dot{\varphi}_{i+1}^e\\
&-\Big(r_i\,(b_i^e + b_{i+1}^e) + (h/2)\,(b_i^e - b_{i+1}^e)\Big)\,\dot{\varphi}_i^e\Bigg) + \dot{\mathfrak{M}}_i^e = 0\,,
\end{aligned} \tag{10}$$

under the hypothesis that the coefficients c_i scale as ψ_i^b in Eq. (3).

The tube is acted upon by prescribing either the applied end couples ($\mathrm{M}_i^e = \mathfrak{M}_i^e(t)$) or the end angles of rotation ($\varphi_i^e = \Phi_i^e(t)$). Typically, we take $\varphi_0^- = 0$, $\varphi_0^+(t) = \Phi(t)$ for a given Φ, and $\mathfrak{M}_i^e = 0$ for all $i > 0$. We then integrate Eqs. (8) and (10) in time, starting from *null* initial conditions for all state variables, except the a-defect densities on the *outermost* wall, where we posit $a_0^e(0) = a_{00}^e$, for given $a_{00}^- > 0$, $a_{00}^+ > 0$.

REFERENCES

1. P. A. Williams, S. J. Papadakis, A. M. Patel, M. R. Falvo, S. Washburn and R. Superfine, *Appl. Phys. Lett.* **82**, 805 (2003).

2. P. A. Williams, S. J. Papadakis, A. M. Patel, M. R. Falvo, S. Washburn and R. Superfine, *Phys. Rev. Lett.* **89**, 255502 (2002).
3. S. J. Papadakis, A. R. Hall, P. A. Williams, L. Vicci, M. R. Falvo, R. Superfine and S. Washburn, *Phys. Rev. Lett.* **93**, 146101 (2004).
4. A. M. Fennimore, T. D. Yuzvinsky, W.-Q. Han, M. S. Fuhrer, J. Cumings and A. Zettl, *Nature* **424**, 408 (2003).
5. B. Bourlon, D. C. Glattli, C. Miko, L. Forró and A. Bachtold, *Nano Lett.*, **4**, 709 (2004).
6. J. C. Meyer, M. Paillet and S. Roth, *Science* **309**, 1539 (2005).
7. R. H. Telling, C. P. Ewels, A. A. El-Barbary and M I. Heggie, *Nature Materials* **2**, 333 (2003).
8. M. Huhtala, A. V. Krasheninnikov, J. Aittoniemi, S. J. Stuart, K. Nordlund and K. Kaski, *Phys. Rev. B* **70**, 045404 (2004).
9. M. Monteferrante, A DFT study of Cr on graphene, with additional material on molecular dynamics, PhD thesis, Università "Roma Tre", (Italy, 2006), pp. iv + 135.
10. A. DiCarlo, M. Monteferrante, P. Podio-Guidugli, V. Sansalone and L. Teresi, How (and why) twisting cycles make individual MWCNTs stiffer, in *Molecular Nanostructures*, eds. H. Kuzmany *et al.*, AIP Conf. Proc. N. 723, (AIP, Melville, NY) pp. 355–358.
11. J. P. Lu, *Phys. Rev. Lett.* **79**, 1297 (1997).

Acknowledgements

We gratefully acknowledge the support of the Italian Group for Mathematical Physics (GNFM-INdAM) and of the Italian Ministry of University and Research (MIUR) through the Project "Mathematical Models for Materials Science". P. P-G also acknowledges the support of the EU Marie Curie Research Training Network MULTIMAT "Multiscale Modelling and Characterisation for Phase Transformations in Advanced Materials" (MRTN-CT-2004-505226).